

# The phase transition in QCD with broken $SU(2)$ flavour symmetry

Rajiv V. Gavai\* and Sourendu Gupta†

*Department of Theoretical Physics, Tata Institute of Fundamental Research,  
Homi Bhabha Road, Mumbai 400005, India.*

## Abstract

We report the first investigation of the QCD transition temperature,  $T_c$ , for two flavours of staggered quarks with unequal masses at lattice spacings of  $1/4T$ . On changing the  $u/d$  quark mass ratio in such a way that  $m_{\pi^0}^2/m_{\pi^\pm}^2$  changes from 1 to 0.78, thus bracketing the physical value of this ratio, we find that  $T_c$  remains unchanged in units of both  $m_\rho$  and  $\Lambda_{\overline{MS}}$ .

arXiv:hep-lat/0208019v1 14 Aug 2002

---

\*Electronic address: gavai@tifr.res.in

†Electronic address: sgupta@tifr.res.in

Lattice simulations of QCD with dynamical quarks aim to generate weights for the Euclidean path integral

$$Z = \int \mathcal{D}U \exp[-S] \text{Det}M_u \text{Det}M_d, \quad (1)$$

discretised on a space-time lattice. Here  $U$  are gauge fields which enter the action  $S$  and the determinants of the Dirac operator  $M$  for both  $u$  and  $d$  flavours. This leads to the well-known doubling problem in the chiral limit. Several solutions are known and have been used fairly extensively. One is to work with Wilson quarks, for which chiral symmetry is broken through an irrelevant operator at finite lattice spacing and recovered in the continuum. Among the new solutions is the domain wall definition of quarks [1] in which the theory is extended to five dimensions, and by suitable tweaking of this extended action chiral symmetry is obtained on a four dimensional slice through the lattice when the length of the fifth dimension is sent to infinity. Another recently discovered solution is the overlap definition [2], in which chiral symmetry is intact but its generator and the Dirac operator are non-local at finite lattice spacing, but become local in the continuum.

In this study we used the solution popular in finite temperature studies— staggered quarks. These have an exact continuous chiral symmetry at all lattice spacings,  $a$ , and in the continuum limit give 4 degenerate flavours in 4-dimensions. Two degenerate flavours are obtained by the prescription

$$\text{Det}M_u \text{Det}M_d = \left( \text{Det}M_{stag} \right)^{1/2}, \quad (2)$$

where  $M_{stag}$  is the determinant for a single staggered quark field.

In this paper we introduce two staggered quark fields and define two flavours by the prescription

$$\text{Det}M_u \text{Det}M_d = \left( \text{Det}M_{stag(u)} \text{Det}M_{stag(d)} \right)^{1/4}, \quad (3)$$

which we call 1+1 flavours. When the two quark masses are degenerate, this definition gives the same weight in the partition function of eq. (1) as the definition in eq. (2). The new prescription allows us to handle problems involving breaking of vector  $SU(2)$  flavour symmetry, such as unequal masses for the  $u$  and  $d$  quarks (which we explore in this paper) and putting isovector chemical potential on the lattice [3].

Our strategy here is to proceed in two steps— first to compare 2 flavours with 1+1 flavours of degenerate light quarks, and next to lift the degeneracy by giving unequal masses to the

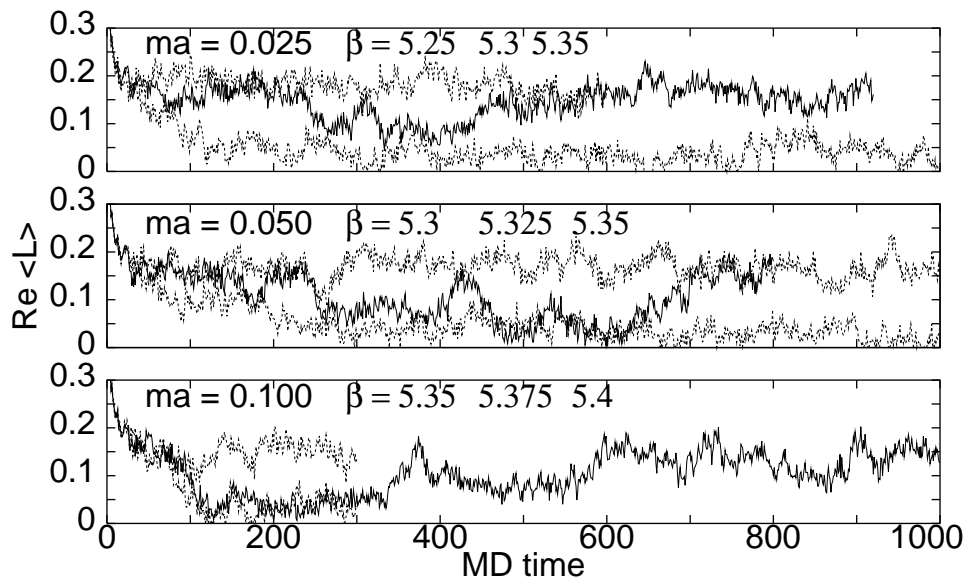


FIG. 1: Run time histories of  $\langle \text{Re} L \rangle$  on  $4 \times 8^3$  lattices for 1+1 flavours of staggered quarks at several couplings close to  $\beta_c$ . The dark lines correspond to runs at  $\beta_c$ . Of the two lighter lines, the upper always corresponds to a simulation at  $\beta > \beta_c$ . The thermalisation time is not more than 100 trajectories.  $\beta_c$  can be easily identified by eye from the long autocorrelation time  $\tau$ .

quarks (we shall use the notation  $\bar{m} = (m_u + m_d)/2$ ). In each case we simulate the finite temperature theory on  $4 \times 8^3$  lattices for several  $\bar{m}$ . We study the real part of the Wilson line,  $\langle \text{Re} L \rangle$ , the quark condensate,  $\langle \bar{\psi}\psi \rangle = (\langle \bar{u}u \rangle + \langle \bar{d}d \rangle)/2$  and the related susceptibilities

$$\begin{aligned} \chi_L &= V \left( \langle (\text{Re} L)^2 \rangle - \langle \text{Re} L \rangle^2 \right), \\ \chi_F &= V \left( \langle (\text{Tr} M^{-1})^2 \rangle - \langle \text{Tr} M^{-1} \rangle^2 + \langle (\text{Tr} M^{-2}) \rangle \right) = \chi_m + \chi_\pi, \end{aligned} \quad (4)$$

where  $\chi_m$  is the chiral susceptibility defined in [4] and  $\chi_\pi$  is the pion susceptibility of [5].  $\chi_F$  has the simple stochastic estimator [6]

$$\chi_F/V = \langle \overline{(r^\dagger M^{-1} r)^2} \rangle - \langle \overline{r^\dagger M^{-1} r} \rangle^2, \quad (5)$$

where each  $r$  is a complex random vector with each component drawn from a Gaussian distribution of unit width and the bar denotes an average over such an ensemble. We also study the integrated autocorrelation time,  $\tau$  [7], of  $\langle \text{Re} L \rangle$  and  $\langle \bar{\psi}\psi \rangle$ , measured self-consistently over runs of length of at least  $30\tau$ .  $\beta_c$  can be defined by peaks in  $\chi_L$ ,  $\chi_F$  and

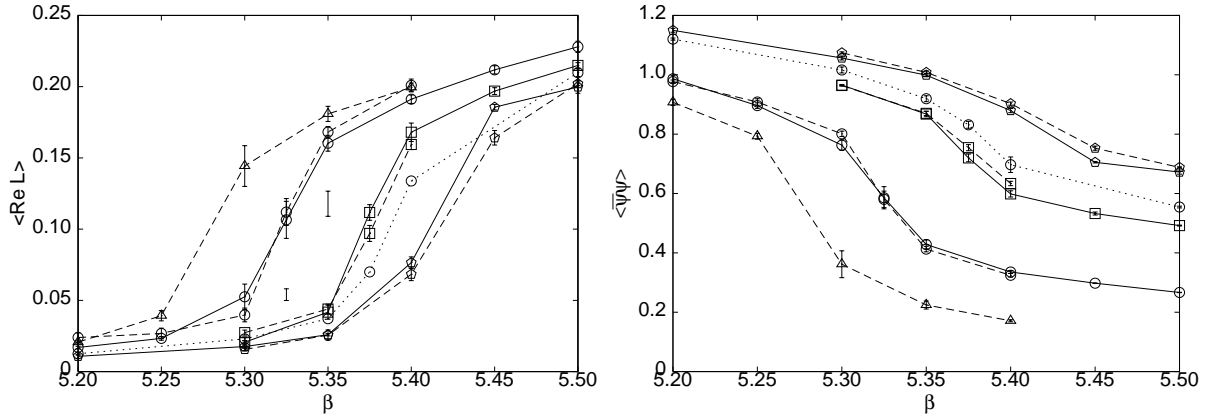


FIG. 2:  $\langle \text{Re} L \rangle$  and  $\langle \bar{\psi} \psi \rangle$  as functions of  $\beta$  for  $\bar{m} = 0.025$  (triangles) 0.05 (circles), 0.1 (boxes) and 0.15 (pentagons). The lines join centers of the measured data points. There is no significant difference between the measurements with  $m_d/m_u = 1$  (dashed lines) and 2 (full lines). However, when  $m_d/m_u = 10$  (dotted line), there is a significant shift in  $\beta_c$ .

$\tau$ . Within the accuracy of our determinations, they agree. We also make zero temperature measurements of the plaquette,  $P$ , and the masses of the pion,  $m_\pi$ , and the rho meson,  $m_\rho$ , at  $\beta_c$  on  $8^4$  lattices (we confirm that the lattice is large enough for these measurements by checking that the zero temperature measurements are independent of boundary conditions). The measurement of  $P$  at  $T = 0$  also allows us to extract  $\alpha_s$  [8] and hence to convert  $a$  into a physical length scale in order to extract  $T_c/\Lambda_{\overline{MS}}$ .

Our measurements have been taken at bare quark masses,  $a\bar{m} = 0.15, 0.1, 0.05$  and  $0.025$  for degenerate flavours. For non-degenerate flavours with  $m_d = 2m_u$  we have only worked with the first three values of  $\bar{m}$ . We have also investigated  $m_d = 10m_u$  with  $a\bar{m} = 0.15$ . The simulations have been performed with the Hybrid-R algorithm [9]. This algorithm is based on a molecular dynamics (MD) evolution which treats degenerate 1+1 and 2 flavours differently. Hence, the agreement in the results of these two cases, which we show later, is a good test that the numerical treatment of the discretised MD evolution is free of errors at the level of accuracy we achieve. The trajectory lengths have been taken to be one unit of molecular dynamics time, and the MD equations have been integrated over this range in 100 steps. Some typical run time histories of  $\langle \text{Re} L \rangle$  are shown in Figure 1. Run time histories of other quantities are similar. The slow but large fluctuations visible in some of these runs are typical of critical slowing down, and therefore yield estimates of  $\beta_c$ .

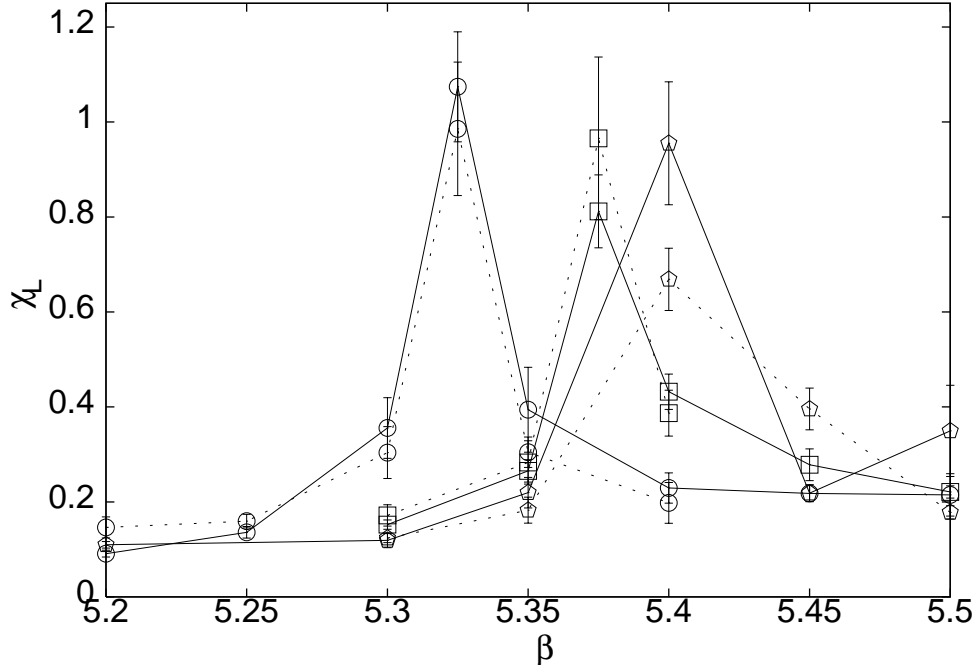


FIG. 3: The Wilson-line susceptibility  $\chi_L$  as a function of  $\beta$  for  $\bar{m} = 0.05$  (circles),  $0.1$  (boxes) and  $0.15$  (pentagons). The lines join centers of the measured data points for  $m_d/m_u = 2$  (full lines) and  $1$  (dotted lines).

Our measurements of  $\langle \text{Re } L \rangle$  and  $\langle \bar{\psi} \psi \rangle$  are collected in Figure 2. Clearly there are no statistically significant differences between the measurements with degenerate quark masses and for  $m_d/m_u = 2$ . From these figures it is also clear that  $\beta_c$  is not sensitive to variation of  $m_d/m_u$  in the range 1–2. From our measurements of masses, detailed later, it turns out this range of bare quark mass ratios includes the range of  $m_{\pi^0}^2/m_{\pi^+}^2$  between 1 and roughly 0.8. Since the physical pion masses [14] yield  $m_{\pi^0}^2/m_{\pi^+}^2 = 0.935$ , which is inside this range, we may conclude that the shift in  $\beta_c$  due to realistic vector  $SU(2)$  flavour symmetry breaking is negligible at the level of accuracy we can reach. A significant downward shift in  $\beta_c$  is seen when the ratio  $m_d/m_u$  is made as large as 10,

The measurements of autocorrelations yield strong peaks, sometimes as high as 300 MD time units, at couplings which we identify as  $\beta_c$ . These runs were extremely time consuming, since some of them required more than  $10^4$  trajectories for reliable estimates of the susceptibilities shown in Figures 3 and 4. These also peaked at the same values of  $\beta$ , and are our primary means for the identification of  $\beta_c$ . Very good agreement between measurements of

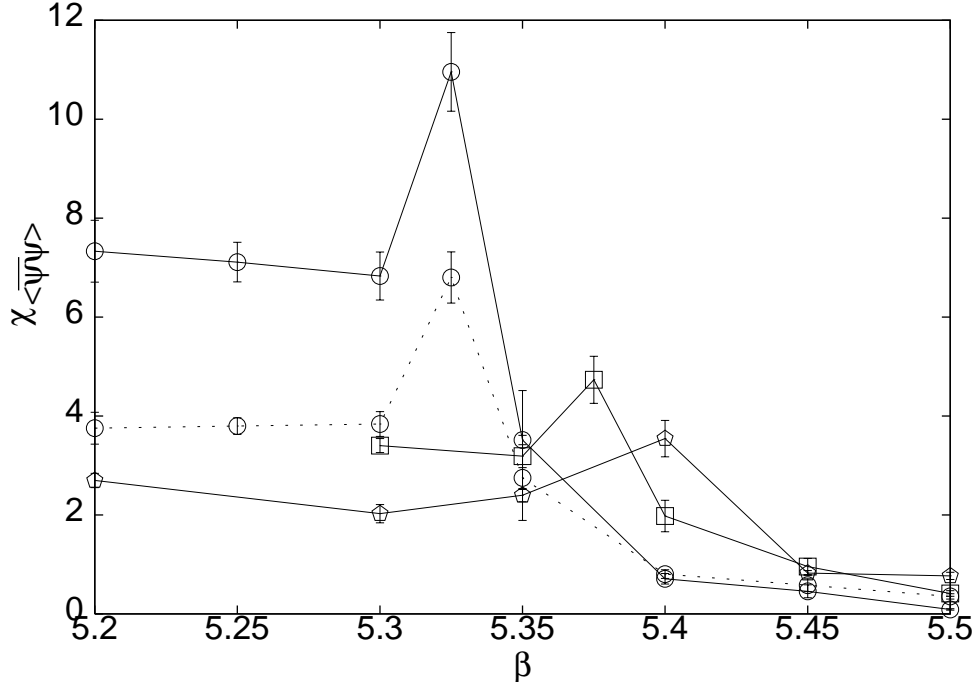


FIG. 4: The susceptibility for the chiral condensate,  $\chi_{\langle\bar{\psi}\psi\rangle}$ , as a function of  $\beta$  for  $\bar{m} = 0.05$  (circles), 0.1 (boxes) and 0.15 (pentagons) and for  $m_d/m_u = 2$ . The lines join centers of the measured data points. The  $\langle\bar{u}u\rangle$  susceptibility is shown except at the lightest  $a\bar{m}$  where the  $\langle\bar{d}d\rangle$  susceptibility is also shown for comparison (dotted line).

$\chi_L$  for  $m_d/m_u = 2$  and 1 indicate that there is no shift in  $\beta_c$ . The only exception is the value of  $\chi_L$  near  $\beta_c$  for  $a\bar{m} = 0.15$ , where the difference can be attributed to the factor two difference in statistics between the runs with  $m_d/m_u = 2$  and 1—the former have both larger statistics and  $\chi_L$ . In Figure 4 we show  $\chi_F$ , which also peak at the same  $\beta_c$ , but unlike  $\chi_L$  have stronger quark mass dependence.

Our estimates of  $\beta_c$  for 1+1 flavours are shown in Table II. Measurements of  $\beta_c$  with the 2 flavour definition of staggered quarks have been made earlier in [10] on  $4 \times 8^3$  lattices with  $a\bar{m} = 0.1, 0.05$  and  $0.025$ . Estimates of  $\beta_c$  have also been made on lattices with  $N_t = 4$  for  $a\bar{m} = 0.025$  and  $0.0125$  in [11]. These earlier results are fully in agreement with our measurements. Recall that studies on fixed volumes cannot decide the order of the transition, or indeed whether the peaking of the susceptibilities are due to a phase transition or a cross-over. That requires a study with varying volumes—a work that is outside the scope of this investigation and left for later.

$a\bar{m}$	$m_d/m_u$		All	3:13	5:11	All (2 mass)
0.025	1	$am_\pi$	0.422 (2)	<u>0.419(4)</u>	0.42 (1)	0.419 (4)
	1	$am_\rho$	<u>1.16(4)</u>	1.4 (2)		
0.05	1	$am_\pi$	0.587 (4)	<u>0.579(6)</u>	0.585 (8)	0.579 (6)
	2	$am_{\pi^+}$	0.588 (2)	0.582(2)	0.583 (5)	<u>0.581 (2)</u>
	2	$am_{\pi^0}$	0.535 (4)	0.521 (3)	0.516 (5)	<u>0.516(4)</u>
	1	$am_\rho$	<u>1.29(5)</u>	1.4 (1)	1.1 (4)	
	2	$am_{\rho^+}$	<u>1.31(5)</u>	1.5 (2)		
	2	$am_{\rho^0}$	<u>1.31(5)</u>	1.5 (3)		
0.10	1	$am_\pi$	0.815 (5)	<u>0.805(9)</u>	0.80 (2)	0.80 (2)
	2	$am_{\pi^+}$	0.818 (3)	<u>0.811(2)</u>	0.811 (3)	0.811 (2)
	2	$am_{\pi^0}$	0.740 (6)	0.717 (3)	0.707 (4)	<u>0.705(6)</u>
	1	$am_\rho$	<u>1.41(5)</u>		1.4 (3)	
	2	$am_{\rho^+}$	<u>1.39(4)</u>		1.4 (2)	
	2	$am_{\rho^0}$	<u>1.38(4)</u>		1.4 (3)	
0.15	1	$am_\pi$	0.973 (2)	0.972 (3)	0.978 (4)	<u>0.970 (3)</u>
	2	$am_{\pi^+}$	0.982 (2)	0.971 (2)	0.968 (3)	<u>0.968 (3)</u>
	2	$am_{\pi^0}$	0.885 (7)	0.852 (4)	0.838 (2)	<u>0.823(7)</u>
	1	$am_\rho$	<u>1.44(3)</u>		1.32 (3)	
	2	$am_{\rho^+}$	<u>1.47(3)</u>		1.47 (5)	
	2	$am_{\rho^0}$	<u>1.45(3)</u>		1.50 (3)	

TABLE I: Meson masses from fits to the form shown in eq. (7) with one or two masses. The range of  $t$  to which the correlation function is fitted is indicated in the column header. The entries for  $m_\pi$  and  $m_\rho$  are measurements with degenerate quark masses. The remainder are for  $m_d = 2m_u$ . We consider the underlined entries to be our best estimates of the meson masses.

We turn now to measurements at zero temperature. For this part of the work we generated configurations on  $8^4$  lattices at the coupling  $\beta_c$  for the value of  $a\bar{m}$  under study. The autocorrelations of  $\langle \bar{\psi}\psi \rangle$  were found to be less than 5 MD time units in all cases, and the thermalisation time was less than 50 trajectories. We discarded the first 50 trajectories and

stored 50 configurations separated by 5 trajectories in each of these simulations.

Meson correlators were computed on the stored configurations by inverting the staggered Dirac operator with appropriate masses. For  $m_u \neq m_d$ , the flavour combinations which give the meson propagators are—

$$\begin{aligned} C_{\pi^+}(r) &= \langle M_u^{-1}(0, r) M_d^{-1}(r, 0) \rangle \\ C_{\pi^0}(r) &= \frac{1}{2} \left[ \langle M_u^{-1}(0, r) M_u^{-1}(r, 0) \rangle + \langle M_d^{-1}(0, r) M_d^{-1}(r, 0) \rangle \right], \end{aligned} \quad (6)$$

where  $r$  labels a point of the lattice with respect to the chosen origin. The correlator for  $\pi^-$  is obtained by flipping the roles of the  $u$  and  $d$  quarks in the expectation value on the right. The analogous combinations for the  $\rho$  have the usual staggered fermion phase factor. The correlators, and hence the masses, for opposite charge states are identical. For degenerate quark masses, the propagators in all the charge states are identical. As usual, these correlators are summed over spatial slices to give the zero momentum propagators.

$a\bar{m}$	$\beta_c$	$m_{\pi^+}^2/m_{\rho^+}^2$	$m_{\pi^0}^2/m_{\pi^+}^2$	$T_c/m_{\rho^+}$	$T_c/\Lambda_{\overline{MS}}$
0.050	5.325 (25)	0.20 (2)	0.78 (2)	0.194 (7)	1.2 (2)
0.100	5.375 (25)	0.34 (2)	0.76 (1)	0.177 (6)	1.3 (2)
0.150	5.400 (25)	0.44 (2)	0.72 (1)	0.172 (4)	1.3 (2)

TABLE II: A summary of our measurements with  $m_d = 2m_u$ . These measurements are statistically indistinguishable from measurements with  $m_d = m_u$  (except for the ratio  $m_{\pi^0}^2/m_{\pi^+}^2$  which is then identically unity). In the limit of physical  $\bar{m}$ ,  $T_c = 175 \pm 6$  from extrapolation of  $T_c/m_{\rho}$  and  $T_c = 167 \pm 9_{-14}^{+15}$  MeV from extrapolation of  $T_c/\Lambda_{\overline{MS}}$ .

Meson masses were obtained by fitting these zero momentum correlators to the form

$$C(t) = A \cosh \left[ m \left( \frac{L}{2} - t \right) \right] + A' \cosh \left[ m' \left( \frac{L}{2} - t \right) \right], \quad (7)$$

or the corresponding single mass formula obtained by dropping the second term. We explored the stability of the fits by changing the range of  $t$  over which the single mass form was fitted, and by comparing the result with the two mass fits.

The detailed comparisons are given in Table I. For the flavour symmetric pion and the  $\pi^+$ , there is a clear stable mass for fits over the range  $3 \leq at \leq 13$ . For the  $\pi^0$  the mass

extracted from the two mass fit lies below that obtained from single mass fits. In all cases we took the lowest estimate to be the value of the mass. For the various  $\rho$ , the fit errors are larger and we accept the single mass fit over the full range of  $t$  as our best estimate of the mass. The 1+1 flavour masses obtained with  $m_u = m_d$  are fully consistent with previous measurements for 2 flavours [10].

We draw attention to the fact that the mass splitting between the charged and uncharged  $\rho$  is not visible within measurement errors, and both these masses are equal to that obtained with degenerate quarks. However, the splitting between the neutral and charged pions is clearly visible. Interestingly, the latter are statistically indistinguishable from the pion mass measured with equal quark masses. Breaking  $SU(2)$  flavour symmetry only results in lowering the  $\pi^0$  mass.

From our extraction of  $am_\rho$ , we extracted the ratio  $T_c/m_\rho = 1/N_t am_\rho$ . These estimates are collected in Table II. The ratio  $T_c/\Lambda_{\overline{MS}}$  increases marginally as  $a\overline{m}$  decreases, due to the small decrease in the measured values of  $am_\rho$ . We have extrapolated these estimates to the values of  $a\overline{m}$  for which the physical value of  $m_\pi/m_\rho$  is obtained, through the form—

$$m_\rho = a + b\overline{m} + \dots \quad (8)$$

For the value of  $a\overline{m}$  where the physical value of  $m_\pi/m_\rho$  is obtained, we find  $T_c/m_\rho = 0.227 \pm 0.008$ . This gives  $T_c = 175 \pm 6$  MeV. Mutually consistent values of  $T_c$  are obtained using the 2-flavour data of [10], and our 1+1 flavour data with  $m_d/m_u = 1$  as well as 2.

Alternatively, the lattice spacing can be traded for  $\Lambda_{\overline{MS}}$  by using our measurements of the plaquette,  $P$ , to extract the running coupling,  $\alpha_s$ , and using this in the 2-loop  $\beta$  function. This procedure was introduced in [8] and later used to determine  $T_c/\Lambda_{\overline{MS}}$  from the 2 flavour data for realistic quark masses in [12]. With such an analysis, the values of  $T_c/\Lambda_{\overline{MS}}$  extracted from our measurements in the 1+1 flavour case agree completely with the previous values at the same  $a\overline{m}$ . Extrapolation of our 1+1 flavour results to quark masses which give the correct value of  $m_\rho/\Lambda_{\overline{MS}}$ , yield  $T_c/\Lambda_{\overline{MS}} = 0.49 \pm 0.02$ , as in [12]. Then, using the 2-loop value of  $\Lambda_{\overline{MS}} = 343_{-28}^{+31}$ , as appropriate below the charm quark threshold [14], we obtain  $T_c = 167 \pm 9_{-14}^{+15}$  MeV (where the first error comes from  $T_c/\Lambda_{\overline{MS}}$  and the second from  $\Lambda_{\overline{MS}}$ ). The two estimates of  $T_c$  are totally compatible with each other, and also from other estimates using improved actions [15].

The above method depends on the expansion of  $P$  at  $T = 0$  in a series in  $\alpha_s$ . Since this

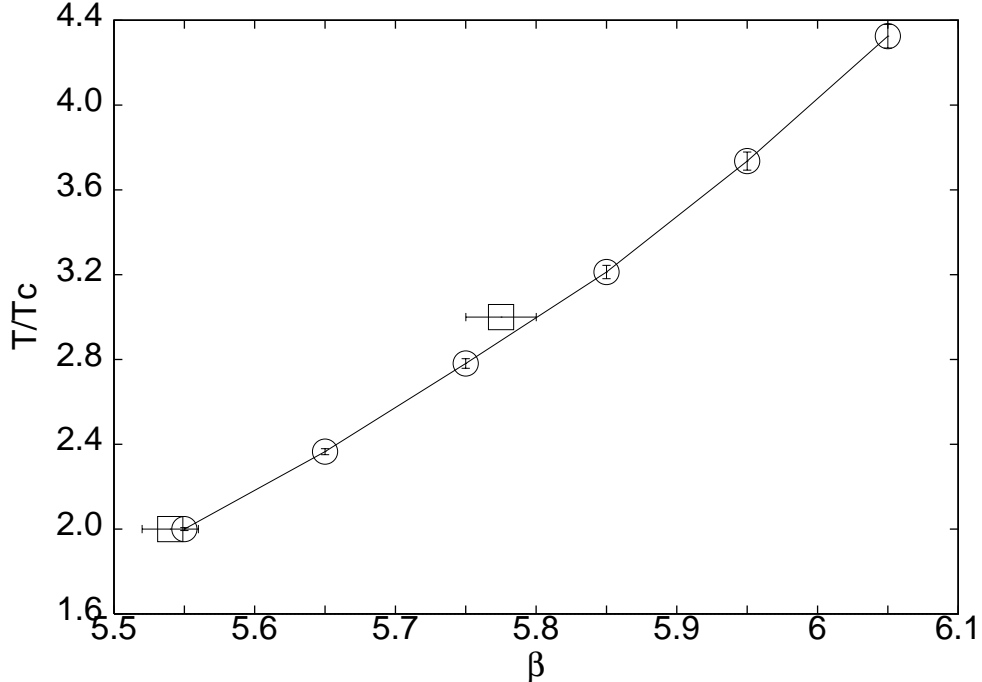


FIG. 5: The relation between the lattice spacing and  $\beta$ , shown in terms of the dependence of  $T/T_c$  on  $\beta$  for  $N_t = 4$  lattices. The circles denote estimates from measurements of  $P$ . Squares denote estimates from measurements of  $\beta_c$  on lattices with different  $N_t$  [16].

is scheme dependent [13], the extraction of  $T_c/\Lambda_{\overline{MS}}$  can have large uncertainties if the cutoff is large. To estimate these, we have extrapolated the temperature scale to smaller lattice spacings and compared to direct measurements of the scale. At the smallest  $\overline{m} = 0.025/a$  we have made a few  $T = 0$  runs at larger  $\beta$  to estimate the lattice spacing through a measurement of  $P$ . Since the lattice spacing,  $a$ , is an outcome of this computation, a series of runs is needed to tune  $\overline{m}$ . The scale determined in this way can be converted into a temperature scale for simulations with  $N_t = 4$  at the corresponding  $\beta$ . This is shown in Figure 5. The temperature scale for  $N_t = 4$  can also be calibrated by direct measurements of  $\beta_c$  at larger  $N_t$ . For 2 flavours of quarks and  $\overline{m} = 0.025/a$ , such measurements have been performed [16]. These results are also plotted in Figure 5. The good agreement between the two methods of setting the scale implies that the lattice spacings are fine enough for 2-loop scaling to work. As a result, we expect that  $T_c/\Lambda_{\overline{MS}}$  obtained here are relevant to the continuum limit.

The major remaining uncertainties are in the extrapolation to zero quark mass, and in

possible power corrections in  $a$  to various quantities we have measured. The question of the order of the phase transition needs a finite size scaling study and has not been addressed here. A detailed study of these issues lies outside the scope of this paper, and is left to the future.

- 
- [1] D. Kaplan, *Phys. Lett.*, B 288 (1992) 342;  
Y. Shamir, *Nucl. Phys.*, B 406 (1993) 90.
  - [2] H. Neuberger and R. Narayanan, *Phys. Rev. Lett.*, 71 (1993) 3251.
  - [3] J. B. Kogut and D. K. Sinclair, hep-lat/0201017; S. Gupta, hep-lat/0202005.
  - [4] S. Aoki *et al.*, *Phys. Rev.*, D 57 (1998) 3910;  
E. Laermann, *Nucl. Phys. Proc. Suppl.*, 63 (1998) 114.
  - [5] S. Gupta, *Phys. Lett.*, B 286 (1992) 112.
  - [6] R. V. Gavai *et al.*, *Phys. Rev.*, D 65 (2002) 054506.
  - [7] For the definition of the integrated autocorrelation time, see, for example, A. Billoire *et al.*, *Nucl. Phys.*, B 358 (1991) 231.
  - [8] G. P. Lepage and P. B. Mackenzie, *Phys. Rev. D* 48 (1993) 2250.
  - [9] S. Gottlieb *et al.*, *Phys. Rev. D* 35 (1987) 2531.
  - [10] S. Gottlieb *et al.*, *Phys. Rev. Lett.*, 59 (1987) 1513.
  - [11] M. Fukugita *et al.*, *Phys. Rev. Lett.*, 65 (1990) 816;  
M. Fukugita *et al.*, *Phys. Rev.*, D 42 (1990) 2936.
  - [12] S. Gupta, *Phys. Rev.*, D 64 (2001) 034507.
  - [13] G. Martinelli *et al.*, *Phys. Lett.*, 100 B (1981) 485; S. J. Brodsky, G. P. Lepage and P. B. Mackenzie, *Phys. Rev. D* 28 (1983) 228.
  - [14] Particle Data Group, *Eur. Phys. J.*, C 3 (1998) 1.
  - [15] F. Karsch *et al.*, *Nucl. Phys.*, B 605 (2001) 579; A. Ali Khan *et al.*, *Phys. Rev.*, D 63 (2001) 034502.
  - [16] S. Gottlieb *et al.*, *Phys. Rev.*, D 47 (1993) 3619; C. Bernard *et al.*, *Phys. Rev.*, D 54 (1996) 4585.